Sensors and Materials, Vol. 38, No. 2 (2026) 713–723
MYU Tokyo

S & M 4341

Carbon-fiber-reinforced Foam/Carbon-fiber-reinforced Plastic Hybrid Structure Optimized for Mammography with High X-ray Transmittance

Toru Negishi,[1] Kiyomitsu Shinsho,[1*] Kazuya Mori,[1]
Masato Honma,[2] Hiroaki Matsutani,[2] and Tomohiro Takehara[3]

[1]Tokyo Metropolitan University, 7-2-10 Higashi-Ogu, Arakawa-ku, Tokyo 116-8551, Japan
[2]Composite Materials Research Laboratories, Toray Industries, Inc.,
1515, Tsutsui, Masaki-cho, Iyogun, Ehime 791-3193, Japan
[3]Advanced Composites Technical Dept., Toray Industries, Inc., 9-1, Oe-cho, Minato-ku, Nagoya 455-8502, Japan

(Received October 7, 2025; accepted December 8, 2025)

Keywords: carbon-fiber-reinforced foam (CFRF), X-ray transmittance, flexural stiffness, mammography, dose reduction

To reduce patient radiation exposure in mammographic imaging, we investigated the mechanical and radiographic properties of a newly developed carbon-fiber-reinforced foam (CFRF) and its hybrid structures with conventional carbon-fiber-reinforced plastic (CFRP). Flexural stiffness and X-ray transmittance were evaluated for multiple composite designs using three-point bending and transmission measurements under mammographic conditions. The CFRF-only specimen demonstrated a 5% improvement in transmittance and a 25% increase in flexural stiffness compared with CFRP. Moreover, the CFRF thickness can be reduced from 3.4 to 3.2 mm while maintaining equivalent stiffness. Among all designs, the CFRP/CFRF/CFRP sandwich structure achieved the highest transmittance (94.1%) and superior stiffness at the same thickness as conventional CFRP, indicating its high suitability for mammographic platforms. The results suggest that CFRF-based composites offer promising potential to reduce radiation dose while maintaining image quality in breast imaging systems.

1. Introduction

Mammography is an essential diagnostic technique for the early detection of breast cancer, utilizing differences in X-ray attenuation to visualize the internal tissue structure of the breast. However, since the breast consists of adipose and glandular tissues, and their mass attenuation coefficients differ only slightly, the sensitivity of cancer detection decreases, particularly in dense breasts.(1) To address this issue, digital breast tomosynthesis (DBT) has been developed(2) and covered by insurance in Japan since June 2024. However, while DBT improves diagnostic performance, concerns regarding the increased radiation dose to highly radiosensitive glandular tissue remain, necessitating further dose reduction measures.

*Corresponding author: e-mail: shinsho@tmu.ac.jp
https://doi.org/10.18494/SAM5995

ISSN 0914-4935
https://myukk.org/

One major approach to reducing radiation exposure in mammography has been improving the sensitivity of X-ray detectors. The technology has evolved from screen-film mammography to computed radiography, and further to flat panel detectors, resulting in a decrease in mean glandular dose. Additionally, in Japan, the introduction of diagnostic reference levels has promoted the optimization of medical radiation exposure.[3–11]

Another approach to dose reduction is improving X-ray transmission efficiency. In breast imaging, low-energy X-rays are used to enhance subject contrast, making the material of X-ray filters, cassettes, and compression plates critical. Traditionally, carbon-fiber-reinforced plastic (CFRP), which has high X-ray transparency, has been used in cassettes, contributing to dose reduction.[12,13] For compression plates, early models used a collimator-based compression method, which was later replaced with polymethyl methacrylate (PMMA) for safety reasons. Subsequently, polycarbonate and resin have also been adopted. However, there has been little advancement in improving the radiation transparency of compression plate materials, and significant innovations have not been observed for many years.

In this study, we focused on a newly developed carbon-fiber-reinforced foam (CFRF). Compared with conventional CFRP, CFRF is characterized by its lightweight yet high stiffness, making it a promising material for compression plates that can reduce radiation exposure to the breast while maintaining image quality. Previous studies have demonstrated that combining CFRF-based lightweight foam with traditional CFRP enhances rigidity and stiffness. However, the optimal combination conditions of CFRP and CFRF for the breast support table in mammography systems remain unclear.[14]

The novelty of this study lies not in developing a new raw material, but in optimizing hybrid combinations of a commercially available CFRP and a newly developed CFRF for mammographic applications. Although CFRP materials (F6347B-05P and P3442S-10) are commercial products, the CFRF (T700S/PP) is a prototype ultra-lightweight carbon-fiber-reinforced foam provided by Toray Industries. In this study, we focus on the systematic evaluation of flexural stiffness and X-ray transmission for various hybrid configurations (canape and sandwich structures) to achieve both high rigidity and high radiolucency suitable for mammography compression plates. Such a comparative investigation under clinical mammography beam conditions has not been reported and represents the principal originality of this work.

Therefore, in this study, we investigated the potential for optimizing medical radiation exposure by varying the combination and thicknesses of CFRF and CFRP and comparing their X-ray transmission and mechanical properties. This experimental design aimed to clarify how the integration of high-rigidity CFRP and low-density CFRF can achieve an optimal balance between structural stiffness and X-ray transparency, ultimately contributing to the development of next-generation mammography components with reduced patient exposure.

2. Materials and Methods

In this study, all carbon-fiber-based materials were supplied by Toray Industries, Inc. (Japan). The detailed specifications are as follows.

(1) CFRP (CFRP-only): woven prepreg F6347B-05P (carbon fiber/epoxy resin)

(2) CFRF (CFRF-only): prototype carbon-fiber-reinforced foam composed of T700S/PP, without a commercial model name

(3) Canape structure 1: skin layer – F6347B-05P, core – T700S/PP

(4) Canape structure 2: skin layer – unidirectional prepreg P3442S-10, core – T700S/PP

(5) Sandwich structure: same as (4), with UD-CFRP skins (P3442S-10) and T700S/PP core

All materials were fabricated and provided by Toray Industries under identical processing conditions. The CFRF is an ultra-lightweight carbon-fiber-reinforced foam developed by Toray, consisting of short carbon fibers bonded in a three-dimensional skeleton with a polypropylene binder resin, as described in Refs. 15 and 16.

2.1 CFRP and CFRF

Table 1 shows the characteristics of CFRP and CFRF. Figure 1 shows the relationship between the specific gravity and elastic moduli of CFRP and CFRF.(15,16) CFRP consists of carbon fiber layers impregnated with epoxy resin, with the fibers stacked in different orientations. Its specific gravity ranges from 1.5 to 1.6, and it is characterized by being thin, lightweight, and highly rigid. In contrast, CFRF has a structure where a network of short carbon fibers, separated into monofilaments, forms a skeleton. The intersections of the carbon fibers are bonded, and the skeleton is further stabilized with matrix resin. As a result, most of its volume consists of air, giving it a low specific gravity of 0.2 to 0.6. It is thick, ultra-lightweight, and exhibits high stiffness.

In this study, we examined the combinations of CFRP and CFRF shown in Table 2. These combinations were designed to have stiffness equivalent or higher than that of the CFRP used in the breast support table of conventional mammography systems. Note that "UD-CFRP" refers to a unidirectionally aligned fiber layer.

Table 1
(Color online) Characteristics of CFRP and CFRF.

	CFRP	CFRF
Concept	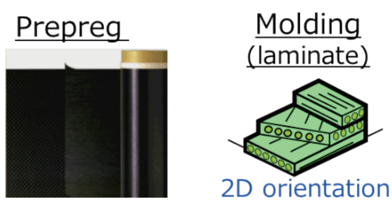	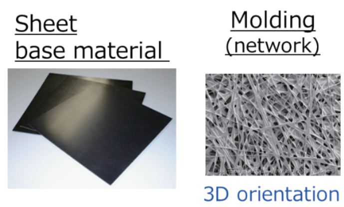
Constitution	CF/epoxy resin (specific gravity: 1.5–1.6)	CF/binder resin/air (specific gravity: 0.2–0.6)
Characteristic	Thin, light weight, High rigidity	Thick, ultra-lightweight, High stiffness

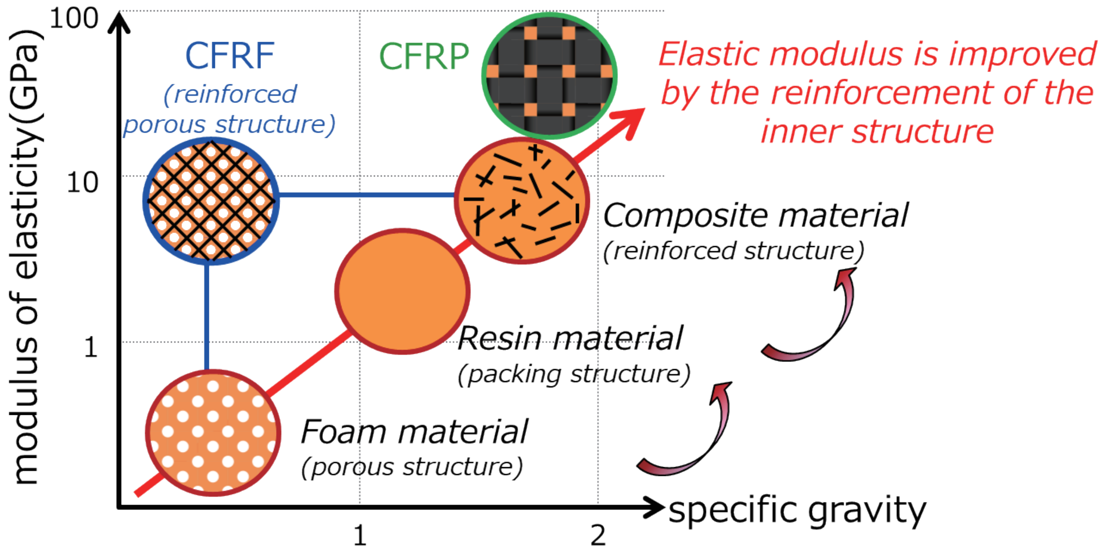

Fig. 1. (Color online) Relationship between specific gravity and elastic moduli of CFRP and CFRF.(15)

Table 2
(Color online) Combinations of CFRP and CFRF.

	Type	Name	Thickness (mm)	Weight per unit area (g/m^2)	Constitution with outline block diagram
①	CFRP	CFRP	1.4	2480	Cloth-CFRP (CF fabric) 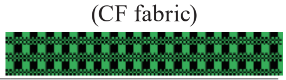
②	CFRF	CFRF	3.4	1200	CFRF 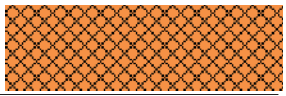
③		Canape structure 1	2.8 UD-CFRP0.2 CFRF2.6	1000	Cloth-CFRP/CFRF 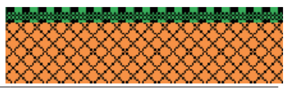
④		Canape structure 2	2.8 UD-CFR P0.2 CFRF2.6	1090	UD-CFRP/CFRF 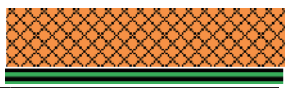
⑤		Sandwich structure	1.4 UD-CFRP0.2 CFRF1.0 UD-CERP0.2	990	UD-CFRP/CFRF / UD-CFRP 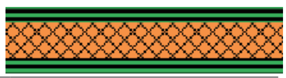

The thicknesses of the CFRF-only and hybrid structures were determined on the basis of the flexural stiffness of the conventional CFRP plate used in existing mammography systems. First, the flexural stiffness of the conventional CFRP (sample ①) was measured experimentally using a three-point bending test according to JIS K7074. Subsequently, the required thicknesses of CFRF and each hybrid configuration were calculated and optimized to achieve stiffness equivalent or higher than that of the reference CFRP. Accordingly, the CFRF-only sample (②) and hybrid designs (③–⑤) were fabricated with those optimized thicknesses to ensure a fair comparison of both stiffness and X-ray transmittance under equivalent mechanical performance conditions. The thickness of the CFRF-only sample (②) was intentionally set to 3.4 mm, which corresponds to the thickness required to achieve flexural stiffness comparable to that of the 1.4-mm-thick conventional CFRP (①). This approach allowed for fair comparison under equivalent stiffness conditions while assessing the effects of density reduction on X-ray transmission characteristics.

Moreover, two canape-type hybrid samples (③ and ④) were prepared to compare the effects of different CFRP skin types on mechanical and radiographic performance characteristics. Sample ③ used a cloth-type CFRP (F6347B-05P) as the skin layer, whereas sample ④ employed a unidirectional CFRP (P3442S-10). This comparison was designed to clarify how the fiber orientation in the outer CFRP layer affects overall flexural stiffness and X-ray transmittance, and to identify the optimal skin configuration for mammographic applications. For the sandwich structure (sample ⑤), UD-CFRP (P3442S-10) was selected as the skin material instead of cloth-type CFRP because its unidirectional fiber alignment provides higher stiffness along the bending axis. In sandwich composites, the skin layers primarily bear tensile and compressive stresses during flexural loading, and therefore, using high-modulus UD-CFRP skins maximizes the overall stiffness while maintaining the high X-ray transparency of the low-density CFRF core.

2.2 Flexural stiffness measurement

Flexural stiffness was evaluated using a three-point bending test based on JIS K7074: “Testing Methods for Flexural Properties of Carbon-fiber-reinforced Plastics”. Figure 2 shows the test configuration. Each sample was supported at two bottom points with a span of 80 mm and loaded at the center using a top contact point. The specimen width was 15 mm. A total of five repeated measurements were conducted for each sample, and the average was calculated. The radii of the upper and lower loading contacts were 5 and 2 mm, respectively. The amount of deflection was recorded under a centrally applied load of 10 N.

2.3 X-ray transmission measurement

X-ray transmittance was measured using the RQA-M2 beam quality, commonly employed in mammography (Mo target/Mo filter at 28 kV, with 2-mm-thick 99.9% pure aluminum as additional filtration). Figure 3 shows the experimental setup. Under this RQA-M2 beam quality, the first half-value layer (HVL) was measured as 0.6 mm Al, corresponding to a mean photon energy of approximately 17–18 keV, which is typical for mammography X-ray beams. The delivered dose was adjusted to maintain a clinically relevant exposure level equivalent to that used in standard mammographic imaging to ensure realistic transmission measurement conditions.

A Titan E Industrial X-ray generator (manufactured by General Electric) was used as the radiation source. Samples were positioned 200 mm from the X-ray tube focal spot. Transmitted

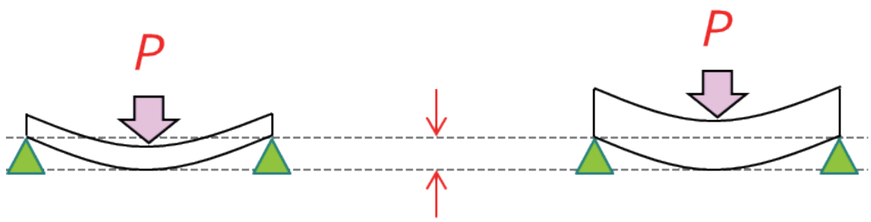

Fig. 2. (Color online) Schematic diagram of three-point bending test.

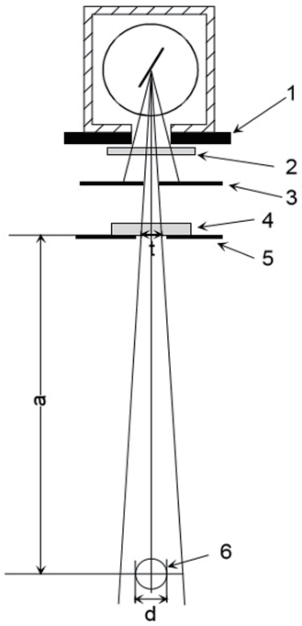

Fig. 3. (Color online) Experimental setup for X-ray transmission measurement. (1: Shutter 2: 2 mm Aluminum Filter 3, 5: 1 mm Lead Collimators 4: Sample 6: Ionization Chamber)

dose was measured using an EMF520R electrometer (EMF Japan) and a TN34069 parallel-plate ionization chamber (PTW). The configuration included a shutter, an aluminum filter, lead collimators, the test sample, and the detector.

3. Results

3.1 Flexural stiffness evaluation

Figure 4 shows the load–deflection curves for the samples listed in Table 2. The conventional CFRP sample (①) exhibited the lowest flexural stiffness, as indicated by the largest deflection under a given load. All CFRF-containing samples demonstrated stiffness equivalent to or higher than that of conventional CFRP.

Among them, the highest stiffness was observed in the CFRF-only sample (②). In the canape structures, CFRF combined with Cloth-CFRP (③) or UD-CFRP (④) showed an equivalent or

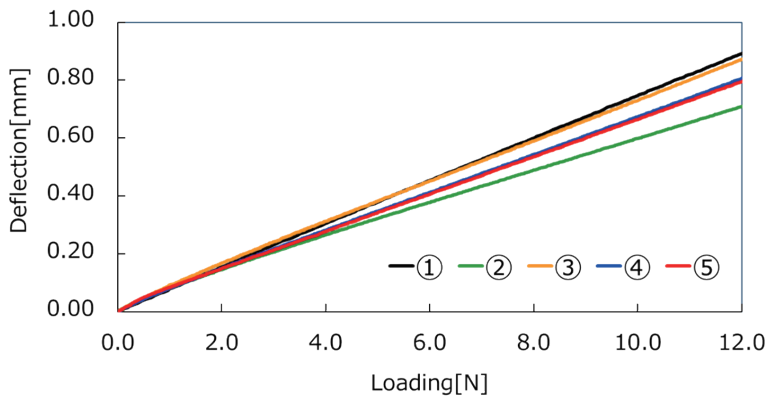

Fig. 4. (Color online) Load–deflection curves. (① CFRP, ② CFRF, ③ Canape Structure 1, ④ Canape Structure 2, ⑤ Sandwich Structure; see Table 2)

smaller deflection and thus an equivalent or higher stiffness than structure ①. Furthermore, when comparing the same overall thickness (1.4 mm) of the CFRP-only sample (①) with that of the sandwich structure (⑤), which has CFRF as the core layer and CFRP as the outer layers, the latter exhibited smaller deflection and thus superior stiffness. For stiffness, the CFRF② and hybrid CFRF-CFRP materials (③,④,⑤) developed in this study exhibited stiffness equivalent or superior to that of the CFRP ① currently used in mammography systems deployed in clinical settings.

In the load–deflection curve, a smaller deflection under the same load indicates higher flexural stiffness. Therefore, the CFRF-only sample (②) actually exhibited the highest stiffness, whereas the CFRP (①) showed the lowest stiffness among the tested materials. The apparent similarity between samples ① (CFRP) and ③ (Canape structure 1) results from the structural balance of the laminate. In sample ③, the CFRP skin layer (F6347B-05P) is thinner than in structure ①, and the CFRF core mainly supports the overall stiffness. Although the CFRF core contributes to reinforcement, its mechanical anisotropy differs from that of the unidirectional CFRP layer used in structures ④ and ⑤, resulting in slightly lower flexural stiffness. Consequently, the total flexural stiffness of sample ③ appears close to that of sample ①, while samples ④ and ⑤ clearly show higher stiffness.

The difference in stiffness between UD-CFRP and cloth-type CFRP arises from their fiber arrangement. The UD-CFRP (P3442S-10) aligns fibers in one direction, efficiently supporting bending loads along the fiber axis, which results in higher stiffness. In contrast, the cloth-type CFRP (F6347B-05P) has woven fibers oriented in two perpendicular directions, providing isotropic reinforcement but reducing the effective modulus in any single direction. Consequently, structures using UD-CFRP skins (④ and ⑤) exhibited a higher stiffness than those using cloth-CFRP (③).

3.2 X-ray transmittance evaluation

Table 3 shows the X-ray transmission rates of the samples listed in Table 2. Transmission was measured relative to air (no sample) and normalized to the transmission rate of conventional CFRP (sample ①).

Table 3
X-ray transmission rates of the samples listed in Table 2.

	① CFRP	② CFRF	③ Canape structure 1	④ Canape structure 2	⑤ Sandwich structure
Average (pC)	263.5	278.9	278.3	277.8	279.5
Standard deviation	0.4899	0.4099	0.4472	0.6189	0.3286
Coefficient of variation (%)	0.1859	0.1470	0.1607	0.2228	0.1176
Transmission rate (%)	88.7	93.9	93.7	93.5	94.1
Relative ratio for ① (%)	100	105.8	105.6	105.4	106.1

The CFRP sample (①) showed a transmission rate of 88.7%, which is already considered high. However, all newly prepared samples demonstrated transmission rates that were more than 5% higher than the CFRP baseline. The sandwich structure (⑤) achieved the highest transmission at 94.1%.

4. Discussion

In this study, we evaluated the potential of CFRF and its hybrid structures with CFRP as alternative materials for mammographic breast support platforms, focusing on both X-ray transmittance and mechanical stiffness.

4.1 Characteristics of CFRF and potential for thickness reduction

Sample ②, consisting of CFRF only, had a thickness of 3.4 mm—greater than the 1.4 mm thickness of the conventional CFRP (①)—yet demonstrated approximately 5% higher X-ray transmission (93.9% vs. 88.7%) and significantly higher stiffness. These results suggest the feasibility of reducing CFRF thickness while maintaining stiffness equivalent to that of CFRP. Our CFRF sample showed an approximately 25% higher stiffness than CFRP, and flexural stiffness (EI) can be estimated from Eq. (1) for rectangular cross sections.

$$EI = E \cdot t^3 \tag{1}$$

Here, E is the Young's modulus of the material and t is the thickness (mm) of the material.

To solve for t_{CFRF} for stiffness equivalent to CFRP, we use

$$t_{CFRF} = 3.4 \cdot \left(\frac{1}{1.25}\right)^{1/3} \approx 3.2\,\text{mm}. \tag{2}$$

This indicates that *CFRF* can maintain equivalent rigidity to a 1.4-mm-thick CFRP plate even when reduced to approximately 3.2 mm in thickness. Furthermore, improvements in X-ray transmission can be anticipated through additional thickness reduction.

4.2 CFRP/CFRF hybrid structures: canape and sandwich

The canape structures (③ and ④) combined CFRF with cloth-CFRP or UD-CFRP. Among them, structure ④ (CFRF with UD-CFRP) demonstrated a higher stiffness than structure ③ (CFRF with cloth-CFRP) at the same thickness. This suggests that UD-CFRP is more suitable than cloth-CFRP as a skin material. The difference in flexural stiffness among these hybrid configurations can be explained by both the number of CFRP skins and their fiber orientation. In sample ③, a single cloth-CFRP skin provides isotropic reinforcement but lower modulus due to the woven crimp structure. In sample ④, the unidirectional CFRP skin aligns fibers along the bending axis, resulting in higher stiffness. Sample ⑤, which incorporates two UD-CFRP skins separated by a CFRF core, further enhances rigidity because the outer skins carry tensile and compressive stresses while the lightweight core resists shear deformation. This double-skin configuration maximizes the moment of inertia, yielding the highest overall stiffness among all tested materials. The sandwich structure (⑤), which consists of CFRP/CFRF/CFRP layers with a total thickness of 1.4 mm, showed the highest X-ray transmission (94.1%). The transmission values for the CFRF-only sample (②) and the sandwich structure (⑤) were 93.9 and 94.1%, respectively. Repeated measurements under identical RQA-M2 conditions showed that the variation in transmittance was within ±0.3%, indicating that this small difference (0.2%) lies within the experimental uncertainty and is therefore not statistically significant. Although their transmittance values are almost identical, their mechanical characteristics differ markedly: the CFRF-only sample has high rigidity, but it needs thickness, whereas the sandwich structure maintained equivalent transparency with substantially higher rigidity, representing a more practical balance between mechanical and radiological performance characteristics. This structure optimally combines the lightweight and high-transmittance properties of CFRF with the mechanical reinforcement of CFRP skins, resulting in a balanced, high-performance material.

The higher X-ray transmittance observed in the sandwich structure (⑤) can be attributed to its internal composition. Although the total thickness (1.4 mm) is the same as that of the solid CFRP plate (①), most of its volume consists of the low-density CFRF core (specific gravity 0.2–0.6), while only thin UD-CFRP skins (each 0.2 mm) cover the surfaces. Because X-ray attenuation is governed by the mass thickness (density × thickness) along the beam path, this configuration markedly reduces the effective mass thickness, resulting in lower absorption and consequently higher transmittance without compromising flexural stiffness. This structural advantage explains why sample ⑤ simultaneously achieved the highest radiolucency and mechanical strength among all tested configurations.

To confirm the validity of the measured X-ray transmission values, we also estimated the expected transmission using the mass attenuation coefficients (μ/ρ) and density of the materials, based on the NIST XCOM database for carbon-based composites. The mass attenuation coefficient of carbon at the mean photon energy of 17–18 keV (corresponding to the RQA-M2 condition) is approximately 0.68–0.72 cm^2/g. Considering the densities of conventional CFRP (1.5–1.6 g/cm^3) and CFRF (0.2–0.6 g/cm^3), the calculated transmissions through 1.4 mm of CFRP and 3.4 mm of CFRF were approximately 89 and 94%, respectively. These theoretical estimates agree with the experimental results (88.7 and 93.9%) within ±3% deviation, confirming that the measured data are consistent with attenuation coefficients and physically reasonable.

Our findings suggest that applying CFRF-based composites to components such as breast support platforms or flat panel detector covers in mammographic systems can potentially reduce patient dose by more than 10%. Moreover, their high stiffness makes them suitable for broader applications, including scatter-reduction grids.

Among the evaluated configurations, the CFRP/CFRF/CFRP sandwich structure offers the best balance of mechanical properties, radiolucency, and practical thickness, making it a strong candidate for clinical implementation.

These findings verify the effectiveness of optimizing hybrid combinations of CFRP and CFRF to achieve both high stiffness and X-ray transparency, confirming the originality and clinical applicability of the proposed design.

In mammography, the breast contains glandular tissue, which has the highest tissue weighting factor in radiation protection; therefore, minimizing the absorbed dose to this tissue is essential. However, because the attenuation coefficients of cancerous and normal glandular tissues are similar, sufficient image contrast is often difficult to achieve. To improve diagnostic accuracy, the breast is compressed and stabilized during imaging, which requires a certain level of mechanical stiffness of the support platform and compression plate while minimizing X-ray absorption. From this clinical perspective, the ideal material for mammographic components should simultaneously provide high X-ray transmittance to reduce patient dose and adequate rigidity to maintain imaging stability.

The results of this study demonstrate that the proposed CFRP/CFRF hybrid structures—especially the sandwich configuration—achieve an optimal balance between these two requirements, showing approximately 94% transmittance and flexural stiffness equivalent to or higher than that of conventional CFRP. Thus, the developed structure can be regarded as close to an ideal material for mammography applications.

5. Conclusions

In this study, we evaluated the performance of a newly developed CFRF and its hybrid structures with CFRP for the purpose of reducing radiation dose while maintaining image quality in mammographic imaging. The CFRF-only sample showed more than 5% higher X-ray transmittance and approximately 25% greater flexural stiffness than the conventional CFRP. Moreover, it was shown that the thickness of CFRF can be reduced from 3.4 to approximately 3.2 mm while maintaining equivalent stiffness. The hybrid structures of CFRF and CFRP—specifically the canape and sandwich configurations—demonstrated superior performance in both stiffness and X-ray transmittance compared with CFRP alone. In particular, the CFRP/CFRF/CFRP sandwich structure achieved the highest transmittance (94.1%), despite having the same overall thickness as the conventional CFRP, indicating its excellent potential as a material for breast support platforms.

These findings suggest that CFRF and its hybrid structures are promising materials for reducing patient dose and improving image quality in mammographic systems. Future studies will focus on further optimization of thickness, the evaluation of durability and moldability, and advancement toward clinical implementation.

Acknowledgments

This study was supported by the Tokyo Metropolitan Medical Engineering Cooperation HUB Organization and funded by Toray Industries, Inc.

Author Contributions

Toru Negishi and Kiyomitsu Shinsho contributed equally to the conception, design, experimentation, data analysis, and writing of this manuscript. Both authors reviewed and approved the final version.

References

1 M. S. Jochelson and M. B. I. Lobbes: Radiology **299** (2021) 36. https://doi.org/10.1148/radiol.2021201948

2 A. Chong, S. P. Weinstein, E. S. McDonald, and E. F. Conant: Radiology **292** (2019) 1. https://doi.org/10.1148/radiol.2019180760

3 G. T. Barnes and I. A. Brezovich: Contrast: Effect of scattered radiation. Breast carcinoma: the radiologists expanded role (Wiley, New York. 1977) pp. 73–81.

4 G. T. Barnes and D. P. Chakraborty: Radiology **145** (1982) 815. https://doi.org/10.1148/radiology.145.3.7146416

5 X. Wu, G. T. Barnes, and D. M. Tucker: Radiology **143** (1991) 143. https://doi.org/10.1148/radiology.179.1.2006265

6 P. S. Rezentes, A. Almeida, and G. T. Barnes: Radiology **210** (1999) 227. https://doi.org/10.1148/radiology.210.1.r99dc35227

7 A. J. Shah, J. Wang, T. Yamada, and L. L. Fajardo: Clin. Breast Cancer **4** (2003) 63. https://doi.org/10.3816/CBC.2003.n.013

8 M. B. Williams, E. A. Krupinski, K. J. Strauss, W. K. Breeden III, M. S. Rzeszotarski, K. Applegate, M. Wyatt, S. Bjork, and J. A. Seibert: J. Am. Coll. Radiol. **4** (2007) 371. https://doi.org/10.1016/j.jacr.2007.02.002

9 K. M. Kanal, E. Krupinski, E. A. Berns, et al.: J. Digit Imaging **25** (2013) 10. https://doi.org/10.1007/s10278-012-9521-3

10 T. Negishi, Y. Koba, K. Shinsho, et al.: Radiol. Phys. Technology. **17** (2024) 765. https://doi.org/10.1007/s12194-024-00823-9.

11 Diagnostic Reference Levels Based on Latest Surveys in Japan - Japan DRLs (2015). chrome-extension://efaidnbmnnnibpcajpcglclefindmkaj/https://j-rime.qst.go.jp/report/DRLhoukokusyoEng.pdf

12 J. Law and A. E. Kirkpatrick: Br. J. Radiol. **62** (1989) 163. https://doi.org/10.1259/0007-1285-62-734-163

13 J. Law and A. E. Kirkpatrick: Brit. Jour. of Radiology **63** (1990) 128. https://doi.org/10.1259/0007-1285-63-746-128

14 Y. Takebe, N. Hirano, M.Honma, K. Shinohara, and T. Fujioka: J. Soc. Mater. Sci. **65** (2016) 555. https://doi.org/10.2472/jsms.65.555

15 M. Honma, A. Tsuchiya, N. Hirano, Y. Nakayama, H. Matsutani, Y. Takebe, N. Imai, T. Takehara, and T. Fujioka: https://www.sankei-award.jp/sentan/jusyou/2022/08.pdf

16 Y. Zhang, B. Xiao, H. Wei, Y. Wang, Y. Wan, and J. Takahashi: J. Sandwich Struct. Mater. **27** (2024) 477. https://doi.org/10.1177/10996362241303054